FACTA UNIVERSITATIS
Series: **Mechanical Engineering** Vol. 13, N^{o} 1, 2015, pp. 47 - 65

FLASH TEMPERATURES GENERATED BY FRICTION OF A VISCOELASTIC BODY

UDC 539

Rainer Heise

Berlin Institute of Technology, Institute of Mechanics, Germany

Abstract. *In this study, we elaborate on the friction between a one-dimensional elastomer and a one-dimensional rigid randomly rough surface. Special emphasis is laid on the energy dissipation in the elastomer. Its subsequent temperature change is under inspection. The elastomer is modeled as a spring and a damper in parallel (Kelvin model) in a one-dimensional substitute model according to the concept of the method of dimensionality reduction (MDR). The randomly rough surface is a self-affine one-dimensional fractal whose Hurst exponent H is varied in an extended range between -1 and 3. In full contact, the temperature shift is dominated by ratio between the typical power dissipated in the elastomer to the power that is led away. It is independent of the normal force and proportional to the sliding speed squared. The flash temperature behavior is discussed for different Hurst exponents.*

Key Words: *Contact Mechanics, Elastomer Friction, Temperature Dependence, Method of Dimensionality Reduction*

1. INTRODUCTION

The roughness of surfaces is considered to be the main source of friction since the seminal work of Bowden and Tabor [1]. Greenwood and Tabor [2] ascribe the frictional behavior of polymers to the deformation losses in the material. Experimentally, Grosch [3] found support for these thoughts by considering friction between rubber and hard specimens with controlled roughness. An insight into the role of rheology [4] and surface roughness [5, 6] in polymer friction was gained in the subsequent years. The concept of the coefficient of friction is used in most works in the field. Hereby, Amontons' laws are implicitly considered to hold: The frictional force is proportional to the normal force and hence the coefficient of friction is independent of the normal force [7, 8]. This is a widely spread law, which is a rather crude model of real frictional systems. It is well-known that both the static and the

Received: January 11, 2015
Corresponding author: Rainer Heise
Institute for Mechanics, Technische Universität Berlin, Straße des 17. Juni 135, D- 10623 Berlin, Germany
E-mail: rainer.heise@tu-berlin.de

dynamic coefficient of friction may be changed by a factor of four depending on geometrical and loading conditions of the tribological system under observation. Schallamach [9] studied elastomer friction experimentally. Deviations from Amontons' laws were under investigation in recent studies [10, 11]. They can originate from macroscopic interfacial dynamics [12, 13, 14] or are related to the contact mechanics of rough interfaces. In this study, we consider the thermodynamic behavior of elastomers due to friction in situations where Amontons' laws lose their validity. Some basic understanding of the frictional response of a viscoelastic body is captured from a simple model: (i) the elastomer is modeled as a Kelvin body, which is completely defined by a constant elastic modulus and a thermally activated viscosity, (ii) the undeformed surface is plain and exhibits no friction microscopically, (iii) the counter body is rigid and has a randomly rough, self-affine fractal surface, (iv) capillarity and adhesion are excluded, (v) the features are investigated in a one-dimensional substitute model.

Although these conditions seem to simplify the situation vastly we still obtain an interesting, non-trivial frictional and thermodynamic behavior of the elastomer. We cannot claim a direct one-to-one correspondence to a full-fledged three dimensional analysis but we see a broad applicability of our results to one-dimensional grounds if the rules put forward in the method of dimensionality reduction (MDR) [15-18] are taken into account. Li et al. [19] provided a study of a one-dimensional rough surface in contact with an elastomer. Dimaki and Popov [20] investigated the temperature dependence of the coefficient of friction for elastomers for an indented cone.

The aim of this note is to study the behavior of an elastomer in contact with a rough surface when temperature shifts in the contacts are admitted.

The MDR maps three-dimensional frictional problems onto one-dimensional ones. Thereby, two different steps have to be taken. Firstly, the contact geometry of the surface has to be taken to a one-dimensional substitute model. Secondly, physical quantities in the contact have to be calculated in the model. Let us review a certain class of surfaces that we employ for our model building.

1.1 Self-affine isotropic surfaces and fractal surfaces

An arbitrary surface may be described by certain statistical key values. We want to mention here the root mean square (RMS) roughness $h \equiv \sqrt{\langle h^2 \rangle}$ and the RMS gradient $\nabla h \equiv \sqrt{\langle (\nabla h)^2 \rangle}$, where $\langle \ldots \rangle$ denotes the ensemble average over several realizations of the system. Both quantities can be related to the power spectrum or autocorrelation function $C(q)$ of the surface under consideration.

In a one-dimensional substitute model these moments of the autocorrelation function can be held constant from an original two-dimensional model

$$\begin{aligned} \langle h^2 \rangle_{1d} &= \int_{-\infty}^{\infty} \mathrm{d}q\, C_{1d}(q) \\ \langle (\nabla h)^2 \rangle_{1d} &= \int_{-\infty}^{\infty} \mathrm{d}q\, q^2\, C_{1d}(q). \end{aligned} \tag{1}$$

Fractal surfaces are self-affine surfaces. This means that the surface looks about the same as the resolution is increased or decreased. There is no natural length scale to be found in this kind of surfaces. Hurst exponent *H* is another quantity to characterize fractal surfaces

$$D_f = 2 - H, \tag{2}$$

where D_f is the fractal dimension of the surface. Under a rescaling of spatial coordinate $x \to \xi x$ height coordinate h changes to $\xi^H h$. The original Hurst exponent ranges from 0 to1. Low values of the Hurst exponent correspond to high volatility: large values of the quantity under consideration have a high probability to be followed by low value. This means that a surface with low Hurst exponent looks rather rugged. High values of the exponent point towards a low volatility, i.e. the values of the physical quantity have a high probability to be followed by another similar value. This corresponds to a smooth surface if height coordinates are under investigation. The range of the Hurst exponent can be further extended.

One-dimensional self-affine isotropic surface h is described by a power spectrum

$$C_{1d}(q) = \hat{c}_0 q_f^{-3} \left(\frac{q}{q_f} \right)^{-2H-1}, \qquad q_i \le q \le q_f \tag{3}$$

with dimensionless strength $\hat{c}_0$ and cut-off wave vectors q_i and q_f.

The RMS roughness and the RMS slope of the surface are computed as

$$\begin{aligned} \langle h^2 \rangle &= \frac{\hat{c}_0 q_f^{-2}}{H} \left(\left(\frac{q_f}{q_i} \right)^{2H} - 1 \right), \\ \langle (\nabla h)^2 \rangle &= \frac{\hat{c}_0}{1-H} \left(1 - \left(\frac{q_i}{q_f} \right)^{2-2H} \right). \end{aligned} \tag{4}$$

Eliminating strength $\hat{c}_0$, the gradient of the surface is given by

$$\langle (\nabla h)^2 \rangle = q_f^2 h^2 \frac{H}{1-H} \frac{1 - \left(\frac{q_i}{q_f} \right)^{2-2H}}{\left(\frac{q_f}{q_i} \right)^{2H} - 1}. \tag{5}$$

Dropping the requirement of the Hurst exponent being in the range [0,1] we can identify three different behaviors of the slope. Keeping in mind $q_f / q_i >> 1$

$$\begin{aligned} \langle (\nabla h)^2 \rangle &= q_f^2 h^2 \frac{-H}{1-H}, \qquad H < 0 \\ \langle (\nabla h)^2 \rangle &= q_f^2 h^2 \frac{H}{1-H} \left(\frac{q_i}{q_f} \right)^{2H}, \qquad 0 < H < 1 \\ \langle (\nabla h)^2 \rangle &= q_i^2 h^2 \frac{-H}{1-H}, \qquad H > 1. \end{aligned} \tag{6}$$

For negative values of H, the short wavelengths dominate the slope. For values of H in the physically most interesting range, the slope is interpolating between the values for long respectively short wave vectors. Finally, for high values of the Hurst exponent the shortest wave number, i.e. the longest wavelength, dominates.

For the generation of a randomly rough surface with the desired properties, we fall back on the Fourier transform

$$h_{1d} = \frac{1}{2\pi}\int_{-\infty}^{\infty} \mathrm{d}q\, B_{1d}(q)\exp[i\phi(x)]. \tag{7}$$

The one-dimensional Fourier coefficients of the surface are proportional to the square root of the power spectrum

$$B_{1D} = \sqrt{\frac{2\pi}{L} C_{1D}}. \tag{8}$$

This choice ensures that the requirements on the roughness and slope are satisfied. Note that B_{1D} has to be symmetric about q_f in order to get a real surface. The randomness of the different realizations of the surface is assured by uniformly distributed random phase ϕ. Here, phase ϕ has to be antisymmetric about q_f to fulfill the reality condition. For a discrete realization, the maximal and minimal wave vectors depend on spatial step dx and system length L

$$q_f = \pi / dx, \qquad q_i = 2\pi / L. \tag{9}$$

The one-dimensional surface is generated as the inverse discrete Fourier transform (DFT). As an example, the DFT of one-dimensional height coordinate h is expressed as

$$h_{1D}(j) = \sum_{k=1}^{N} B_{1D}(k)\exp\left[\frac{2\pi i}{N}(j-1)(k-1)\right]. \tag{10}$$

In order to get a real surface, the symmetry conditions for a discrete realization translate into

$$\begin{aligned} B_{1D}(k) &= B_{1D}(N-k+1) \\ \phi_{1D}(j) &= -\phi_{1D}(N-k+1), \quad k = 1,\ldots,N/2. \end{aligned} \tag{11}$$

We stress that there is a periodicity of $L = Ndx$ due to periodicity feature of the DFT.

2. MODELING

After having described the generation of the one-dimensional substitute surface we now turn to the modeling of the contact itself. In the considered model, two one-dimensional substitute surfaces z and u are moved relative to each other with constant velocity v_0. The surfaces are discretized and the individual sites are labeled by $i = 1,\ldots,N$. In every site i there exists a spring damper combination. This combination is a Kelvin body as shown in Fig. 1.

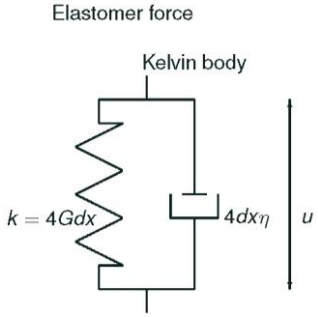

Fig. 1 Kelvin element: Spring with stiffness $k = 2dxG/(1 - \nu)$ in parallel with a damper $\theta = 4dx\eta$

It consists of a spring with stiffness $k = 2\ dx\ G/(1 - \nu)$, which is coupled in parallel with a damper with damping constant$\theta = 4\ dx\ \eta$. The material of the original polymer is described by elastic modulus G and viscosity η. In the one-dimensional model there exists no interaction between neighboring sites. Applied external normal force F_N is held constant during the frictional process. Hence, it is a force controlled process. For simplicity, we employ periodic boundary conditions. One can imagine that the indenter is virtually infinitely many times repeated. Due to the chosen boundary conditions the set-up has spatial periodicity $L = dx\ N$.

Another important ingredient in the model is the contact criterion. The surfaces are considered to be in contact if the coordinate of deformable surface u is larger than the one of rigid surface z:

$$z_i < u_i. \tag{12}$$

From the viscoelastic model mentioned earlier, one can easily find the equation of motion for the Kelvin element at every site $F_{ext} = -k(u - u_0) - \theta\dot{u}$ for some reference coordinate u_0. In terms of discretized variables, the force exerted at each site in contact is

$$f_i = -k\left(u_i + \tau\frac{u_i - u_{i+1}}{dt}\right), \tag{13}$$

where $\tau = \eta/G$ is the relaxation time of the Kelvin element (for incompressible media $\nu = 1/2$). The spring experiences a force according to the deviation from the undisturbed soft surface $u_{0i} = 0$ while the damper exerts a force that is proportional to the rate of change in the deformed surface. We define

$$\bar{v} = \frac{\theta v_0}{kdx} = \frac{\tau}{dt} = \frac{\eta v_0}{Gdx} \tag{14}$$

as the ratio between the time scale of motion $dt = dx/v_0$ and the time scale of the viscoelastic material (relaxation) $\tau = \theta/k = \eta/G$. Between the surfaces, a force acts according to viscoelastic model Eq. (13) if it is in contact. The force is set to zero if surfaces are not in

contact. Negative forces are not considered since this would correspond to adhesive effects which we exclude from our study.

Initially, the rigid surface described by coordinates z_i is generated with a certain given RMS roughness h, system length L, spacing dx and Hurst exponent H. This fixes also the RMS gradient $\nabla z = \sqrt{1/N \sum_{i=1}^{N} ((z_{i+1} - z_i)/dx)^2}$ and cut-off wave vectors q_l and q_f. Note that the mean of z is zero by construction. The moving rigid surface is pressed into the deformable surface in such a way that the given normal force is sustained. At the same time the periodic boundary conditions are enforced. The soft deformed lower surface is now described by coordinate u_i.

The situation is viewed as a stationary system so that all transient features have disappeared. Hence, time step dt for discretization step dx is rather a bookkeeping device. Side step dx is fixed as well as time step dt throughout this study. In particular, this means that spatial derivatives are linked to time derivatives via

$$\frac{d}{dt} = v_0 \frac{d}{dx}. \tag{15}$$

Further on, we denote indices according to the scheme: i all sites, j sites in contact, k sites without contact. The one-dimensional chain can be seen in Fig. 2.

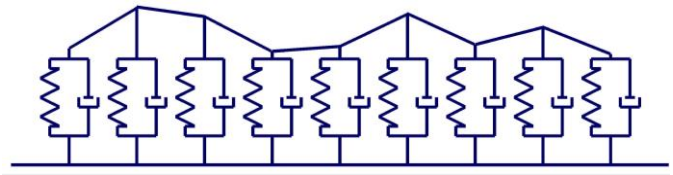

Fig. 2 Chain of discretized Kelvin elements

Imagine we ride along with the indenter to the right. One point of the surface is transferred to a new position. This new position of relaxing surface u_i is calculated according to Eq. (13) without external force. In a continuous description, this leads to a simple ordinary differential equation

$$0 = u - u_0 + \tau \dot{u}. \tag{16}$$

It is solved by

$$u(t) = u(0) \exp\left[-\frac{t}{\tau}\right] \tag{17}$$

after some time t for an undisturbed surface at u_0=0 for some constant $u(0)$.
In discretized coordinates, the solution relates one site to the coordinate one step to the right

$$u_i = u_{i+1} \exp\left[-\frac{dt}{\tau}\right]. \tag{18}$$

This solution corresponds to a free evolution and relaxation of the polymer.

For the deformable surface at a single site, four distinct possible scenarios exist:

(i) The first possibility is a site that is already in contact and remains so. The old coordinate of the element is $u_{j+1}=z_{j+1}$. It evolves freely according to Eq. (18). Its new coordinate fulfills requirement $u_j \geq z_j$ and hence stays in contact. The force at this site in contact is calculated according to Eq. (13). The coordinate of the deformable surface is set to the rigid one, $u_j=z_j$.

(ii) The second possible result of the evolution of a site, which already has been in contact, loses its contact $u_j \leq z_j$. The force acting at this site is set to zero, $f_k = 0$.

(iii) Another outcome of the evolution is that a former free site hits the rigid surface and thus gets into contact $u_j \geq z_j$. Again force f_j in this newly established contact site is calculated in accordance with Eq. (13). Finally, the coordinate is set to the rigid one, $u_j=z_j$.

(iv) The last possibility of evolution is a free contact that stays free. Its coordinate u_k evolves according to the equation of motion Eq. (13) with external force set to zero and reference surface $u_{0k}=0$. Eq. (18) gives the height of surface u_k at this site. There is no force acting between the surfaces at this site, $f_k=0$.

A typical picture of the described situation can be found in Fig. 3.

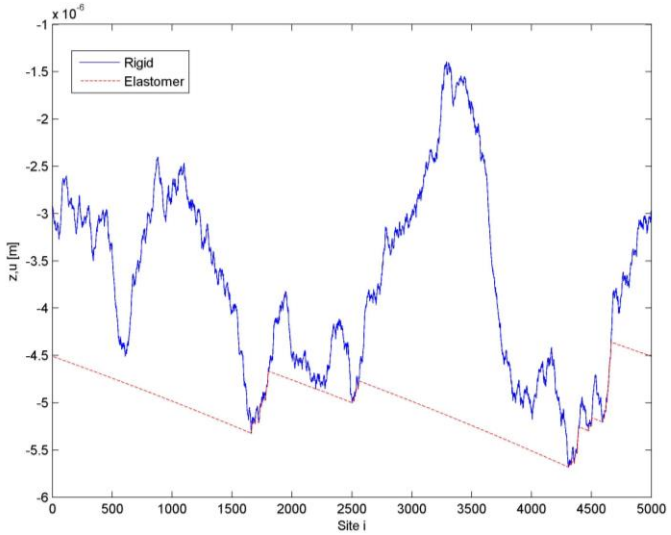

Fig. 3 Typical picture of the surfaces: Rigid rough surface (blue solid) and deformed elastomer (red dashed)

Summing local forces f_i over all the sites yields the total force exerted between the surfaces. This force should equal given normal force F_N. In order to achieve this requirement, the coordinate of the rigid body is adjusted by an overall shift of this surface by a quantity Δz

$$z_i = z_{0i} + \Delta z. \tag{19}$$

The adaptation to the new equilibrium is an iterative process since the contact region changes as well and defines it implicitly.

For the computation of frictional force F_x the tangential force for all sites

$$F_x = \sum_i f_i \nabla z_i = \sum_i f_i \frac{z_{i+1} - z_i}{dx} \tag{20}$$

is calculated. Remember that the sites without contact sustain no force and hence the frictional force equals zero in non-contact sites.

The coefficient of friction is defined as a ratio between the tangential and the total normal force

$$\mu = \frac{F_x}{\sum_i f_i} = \frac{F_x}{F_N}. \tag{21}$$

The contact length is computed as the sum over the number of contact site times the spatial step

$$L_{cont} = \sum_j dx = dx N_{cont}. \tag{22}$$

Another quantity of interest is the surface gradient in contact sites

$$\nabla z_{cont} = \sqrt{\frac{1}{N_{cont}} \sum_j \left(\frac{z_{j+1} - z_j}{dx} \right)^2}, \tag{23}$$

which is a measure for the roughness that is actually experienced by the surfaces.

2.1. Temperature dependence

The temperature dependence of the simulated tribological contact is included in two ways. Firstly, the viscoelastic properties of the material may be changed due to the temperature rise. A detailed analysis [21] reveals the following temperature dependence. Suppose the elastomer can be thought of as an amorphous body consisting of molecules. They usually oscillate in a potential well formed by the surrounding molecules. But there is also the possibility of jumps whose energy is provided by thermal fluctuations within an activation volume. These rarely occurring jumps are the physical reason for a flow in the presence of shear stresses in fluids. Without shear stress, a molecule can jump in any direction with a probability that is proportional to a Boltzmann factor $P \propto \exp[U_0 / k_b T]$ for some temperature T, activation potential U_0, and Boltzmann constant k_b. In absence of a shear stress, there is no macroscopic motion in the fluid. When a shear stress τ_S is imposed onto the system the situation changes in such a way that the potential barriers diminish in the direction of the shear stress by an amount $\tau_S V_0$ for some activation volume. In the direction against the shear stress the potential increases by the same amount. Summarizing the potentials for jumps along and opposite to the shear stress we get

$$\begin{aligned} U_a &= U_0 - \tau_S V_0, \\ U_o &= U_0 + \tau_S V_0. \end{aligned} \tag{24}$$

The activation volumes have the order of magnitude of an atomic volume a^3 where a is the atomic radius. The rate of shear deformation is proportional to the difference in flow of the molecular flow

$$\begin{aligned}\dot{\gamma} &= \frac{dv_x}{dz} = c_o\left(\exp\left[-\frac{U_0-\tau_S V_0}{k_b T}\right]-\exp\left[-\frac{U_0+\tau_S V_0}{k_b T}\right]\right)\\ &= c_1\exp\left[-\frac{U_0}{k_b T}\right]\sinh\left[\frac{\tau_S V_0}{k_b T}\right]\end{aligned} \tag{25}$$

for some (frequency) constant c_1. From this expression, we see a deviation from the behavior of Newtonian fluids. Especially for small shear stress, i.e. $\tau_S V_0/(k_b T)<<1$, we retain only the leading term in the Taylor expansion. Inverting the shear rate expression

$$\dot{\gamma} = \frac{dv_x}{dz} = c_1\exp\left[-\frac{U_0}{k_b T}\right]\frac{\tau_S V_0}{k_b T} = \frac{\tau_S}{\eta} \tag{26}$$

we learn that there exists a prefactor T in addition to the thermal activation Arrhenius term so that the viscosity reads

$$\eta = \frac{k_B T}{c_1 V_0}\exp\left[\frac{U_0}{k_B T}\right]. \tag{27}$$

Referring to a certain state (η_0, T_0) the temperature dependence might be expressed as

$$\begin{aligned}\eta &= \eta_0\frac{T}{T_0}\exp\left[\frac{U_0}{k_B}\left(\frac{1}{T}-\frac{1}{T_0}\right)\right]\\ &= \eta_0\left(1+\frac{\Delta T}{T_0}\right)\exp\left[-\frac{U_0}{k_B T_0}\left(\frac{1}{1+\frac{T_0}{\Delta T}}\right)\right]\approx\eta_0\left(1+\frac{\Delta T}{T_0}\left(1-\frac{U_0}{k_B T_0}\right)\right),\end{aligned} \tag{28}$$

where $\Delta T = T - T_0$. Lyashenko et al. [22] claim that a $\Delta T = 5K$ rise in the temperature might cause a shift of one decade in the frequency of the viscoelastic spectrum. Looking at a temperature $T_0 = 300\ K$ the activation coefficient amounts to 141 in units of $k_b T_0$. Popov [21] says that an increase of the temperature by 30 K leads to a diminishing of the viscosity to a half. This corresponds to an activation energy of 8.67 in units of $k_b T_0$ at $T_0 = 300\ K$. We use the latter value in our calculations.

2.2. Dissipated power

The temperature change originates from the dissipated power in a viscoelastic contact. The energy loss in the viscous part of the element leads to a rise in temperature in the contact. Simple considerations about the heat flow (power flow) in the contact and bulk give rise to a temperature field in the contact.

In three dimensions, heat flow **q** in an isotropic continuum is proportional to the temperature gradient of temperature field T

$$\mathbf{q} = -\lambda \nabla T, \tag{29}$$

according to the Fourier law. Proportionality constant λ is the specific thermal conductivity. The rate of change of the temperature field is governed by the convection-diffusion equation

$$\rho c \frac{\partial T}{\partial t} = -\nabla \cdot \mathbf{q} - \rho c \mathbf{v} \cdot \nabla T + R \tag{30}$$

for a medium of density ρ and specific heat capacity c. The temporal change in temperature is due to the divergence of the heat flow, a convective term due to the motion of the source, and the heat generation from a source R. Including the Fourier equation (29) the rate of change of the temperature for source free materials is then described by the heat exchange equation

$$\rho c \frac{\partial T}{\partial t} = -\nabla \cdot \mathbf{q} - \rho c \mathbf{v} \cdot \nabla T = \lambda \nabla^2 T - \rho c \mathbf{v} \cdot \nabla T. \tag{31}$$

For a stationary situation the time derivative vanishes. Assuming a motion in x direction with velocity v_0, i.e. $\mathbf{v} = (v_0,0,0)$,we obtain an equation for the temperature field

$$\nabla^2 T = \frac{v_0}{\alpha} \partial_x T, \tag{32}$$

where $\alpha = \lambda/(\rho c)$ is the thermal conductance and ∇^2 is the Laplace operator. Its solution consists of a factor that stems from the fundamental solution and a factor describing the motion

$$\delta T = \frac{Q}{2\pi\lambda |\mathbf{x}|} e^{-\frac{v_0}{2\alpha}(|\mathbf{x}|-x)} \qquad \text{for } \mathbf{x} = (x, y, z), \tag{33}$$

Where Q is a point source at $x = 0$. This solution simplifies to the original fundamental solution of the homogeneous Laplace equation if the exponent factor is close to unity, i.e. we get a constraint on the velocity

$$\frac{v_0 dx}{2\alpha} << 1 \tag{34}$$

for characteristic length dx. Especially, at the surface of the half-space $z = 0$ the solution is

$$\delta T = \frac{Q}{2\pi\lambda r} \qquad \text{for } r = \sqrt{x^2 + y^2}, \tag{35}$$

for point-like source Q. If one considers a smeared-out source a distribution

$$|\mathbf{q}| = \frac{q_0}{\sqrt{1 - \left(\frac{r}{a}\right)^2}}, \qquad r < a \tag{36}$$

leads to an isothermal plane at $z = 0$. This is the situation that occurs if two half-spaces are in thermal contact through a circular contact area of radius a in ideal contact. Then the

relationship between the temperature difference between the half-spaces at infinite distance from the contact δT and entire heat flow Q through the passage is given by

$$Q = 4a\lambda^* \delta T, \tag{37}$$

where λ^* is the harmonic mean of the specific thermal conductivities of the half-spaces $1/\lambda^* = 1/\lambda_1 + 1/\lambda_2$. This picture is in accordance with a normal pressure distribution loading an elastic half-space and leading to a constant strain.

Turning to a description in the one-dimensional substitute system we consider the surface as independent element in a Winkler foundation. The thermal conductivity of a single such element is expressed as

$$\Delta\Lambda = 2\lambda^* dx. \tag{38}$$

Through a passage of length $2a$, the amount of

$$\Delta Q = \int_{-a}^{a} j dx = \int_{-a}^{a} 2\lambda^* \delta T dx = 4a\lambda^* \delta T \tag{39}$$

flows in accordance with the three-dimensional result Eq. (37). The heat current through every element j is related to ΔQ and to the temperature difference via

$$j = \frac{\Delta Q}{dx} = 2\lambda^* \delta T. \tag{40}$$

The heat flow in single element of the Winkler foundation is then given by

$$p = 2\lambda^* \delta T dx. \tag{41}$$

Reversing this relation we obtain for the temperature change in one-dimensional substitute model

$$\delta T = \frac{p}{2\lambda^* dx}. \tag{42}$$

For the Kelvin model in a one-dimensional Winkler foundation, the force exerted in one site in contact is given by Eq. (13). The power dissipated in the contact amounts to

$$p_j = f_j \dot{u}_j = -k(u_j + \tau_j \dot{u}_j)\dot{u}_j. \tag{43}$$

In non-contact sites, microscopically energy is dissipated through the relaxation of the Kelvin element. The spring exerts a force on the damper during relaxation. The power dissipated in the element equals the difference of the mechanical energy stored in the spring

$$p_k = \frac{dW}{dt} = \frac{k}{2}\frac{u_k^2 - u_{k-1}^2}{dt}. \tag{44}$$

The temperature itself depends on how this heat is led away. For an element with thermal conductivity λ,

$$\Delta T_j = \frac{2}{\lambda}(Gu_j + \eta_j \dot{u}_j)\dot{u}_j = \frac{k}{2\lambda dx}\left(u_j + \frac{\tau_j}{dt} du_j\right)\frac{du_j}{dt},$$
$$\Delta T_k = \frac{k}{4\lambda dx}\frac{u_k^2 - u_{k-1}^2}{dt} = \frac{Gv_0}{\lambda}\frac{u_k^2 - u_{k-1}^2}{dx}. \tag{45}$$

Keep in mind that the shift in temperature causes a change in the spectral behavior of the elastomer. This is seen in a changing viscosity and hence a shift in relaxation time τ_i. For every site, viscosity η_i. is adapted to temperature T_i in this contact. For points in contact, the change of viscosity leads to a different force experienced by the surface. In this way the entire contact configuration has to be adjusted to the new temperature.

3. Results and Discussion

Numerical simulations have been carried out for different ranges of the parameters involved. The viscosity is chosen to be $\eta_0 = 10^6 Pa\ s$, the modulus $G = 10^6\ Pa$, the thermal conductivity $\lambda = 0.13\ W/m/K$. The normal forces are varied logarithmically in a range from $10^{-4}\ N$, to 20 N, the sliding velocity from $2\ 10^{-8}\ m/s$ to $2\ 10^{-2}\ m/s$. The geometry is described by 5000 steps of with $dx = 2\mu m$ and a roughness $h = 1\mu m$. The Hurst exponent is extended to a range of [-1,3]. In Fig. 4, the coefficient of friction as a function of both velocity and normal force is shown. The viscosity is adapted to the temperature in the contact sites in an iterative process.

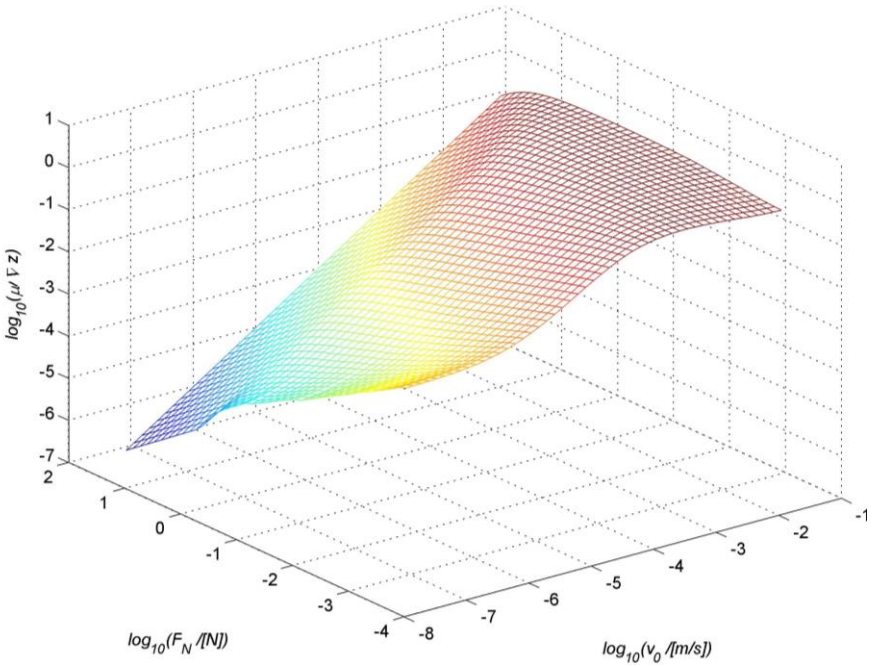

Fig. 4 Coefficient of friction normalized by the RMS slope as a function of velocity and

normal force in logarithmic scale at $H = 0.7$

3.1. Full contact

If the surfaces are pressed with sufficiently high normal force against each other and the velocity is simultaneously rather low a full contact between the surfaces is established. In this situation, several quantities including the temperature can be estimated analytically. The mathematical condition of full contact is

$$u_j = z_j, j = 1,\ldots,N. \tag{46}$$

Therefore, in all the expressions regarding the deformable surface it can be substituted by the unchanged rigid one. Especially, the force in every site is given by

$$f_j = -k(u_j + \tau_j \dot{u}_j) = -k\left(\frac{z_j + z_{j+1}}{2} + \tau_j \frac{v_0}{dx}(z_j - z_{j+1})\right). \tag{47}$$

The averaging of the elastic force is introduced to avoid finite size effects and account for periodicity of the model. The sum of site forces sums up to the normal force

$$F_N = \sum_j f_j = -\sum_j k\left(\frac{z_j + z_{j+1}}{2} + \tau_j \frac{v_0}{dx}(z_j - z_{j+1})\right) = -kN\bar{z}, \tag{48}$$

where $\bar{\chi} = 1/N\sum_j \chi_j$. Hence, the mean value of the rigid profile, i.e. the indentation, is

$$\bar{z} = -\frac{F_N}{kN} = -\frac{F_N}{4GL}. \tag{49}$$

The parameter

$$\frac{\bar{z}}{h} = \frac{F_N}{4GLh} \equiv \frac{\bar{F}}{N}. \tag{50}$$

encodes the relation between indentation and roughness of the surface. We have introduced the dimensionless variable

$$\bar{F} \equiv \frac{F_N}{4Gdxh}. \tag{51}$$

For the frictional force, one encounters the following picture

$$\begin{aligned} F_x &= \sum_j f_j \nabla z_j = f_j \frac{z_{j+1} - z_j}{dx} = \sum_j k\left(\frac{z_j + z_{j+1}}{2} + \tau_j \frac{v_0}{dx}(z_j - z_{j+1})\right)\frac{z_j - z_{j+1}}{dx} \\ &= kv_0 \sum_j \tau_j \frac{(z_j - z_{j+1})^2}{dx^2} = kN\tau\overline{\nabla z^2} = 4Lv_0\eta_0\overline{\nabla z^2} \end{aligned} \tag{52}$$

if one assumes that relaxation time τ_j is approximately the same for all the sites. This is appropriate in the first estimate. The power in every site is found by looking at product of the force at this site and the rate of change of the surface

$$p_j = f_j \dot{u}_j = f_j \frac{z_j - z_{j+1}}{dt} = f_j v_0 \frac{z_j - z_{j+1}}{dx}. \tag{53}$$

Translating this to a temperature shift yields

$$\Delta T_j = T_j - T_0 = \frac{p_j}{2\lambda dx}. \tag{54}$$

For the averaged temperature change, we get

$$\begin{aligned}
\overline{\Delta T} &= \frac{1}{N}\sum_j \Delta T_j = \frac{1}{2\lambda N dx}\sum_j p_j \\
&= \frac{1}{2\lambda N}\sum_j k\left(\frac{z_j + z_{j+1}}{2} + \tau_j \frac{v_0}{dx}(z_j - z_{j+1})\right) v_0 \frac{z_j - z_{j+1}}{dx} \\
&= \frac{k v_0^2}{2\lambda N dx}\sum_j \tau_j \frac{(z_j - z_{j+1})^2}{dx^2} \\
&= \frac{4G dx v_0^2}{2\lambda N dx}\sum_j \frac{\eta_j}{G}\frac{(z_j - z_{j+1})^2}{dx^2} \\
&= \frac{2v_0^2}{\lambda N}\sum_j \eta_0\left(1 + \frac{\Delta T_j}{T_0}\right)\exp\left[-\frac{U_0}{k_B T_0}\left(\frac{1}{1 + \dfrac{\Delta T_j}{T_0}}\right)\right]\frac{(z_j - z_{j+1})^2}{dx^2}.
\end{aligned} \tag{55}$$

Assuming that the temperature shift is about the same at every site $\overline{\Delta T} \approx \Delta T_j$ and that this shift is small $\overline{\Delta T} << T_0$ we find an estimate for the temperature shift at full contact

$$\frac{\overline{\Delta T}}{T_0} = \frac{1}{\dfrac{\lambda T_0}{2v_0^2 \eta_0 \overline{\nabla z^2}} + \dfrac{U_0}{k_B T_0} - 1} \tag{56}$$

From this expression we learn that there are several possible contributions. The first part of the sum in the denominator is the ratio between the typical power dissipated in the viscous material and the power led away. The second part gives a contribution from the thermal activation of the material. Depending on the choice of the parameters the temperature shift can be tuned. In Fig. 5, the proportionality of the temperature shift to the squared velocity is shown at low values of velocity. At these values the surfaces are in full contact. At higher velocities the number of contacts decreases until the number of contacts diminishes to single ones. In this region, it is more sensible to focus on the flash temperature in single contacts.

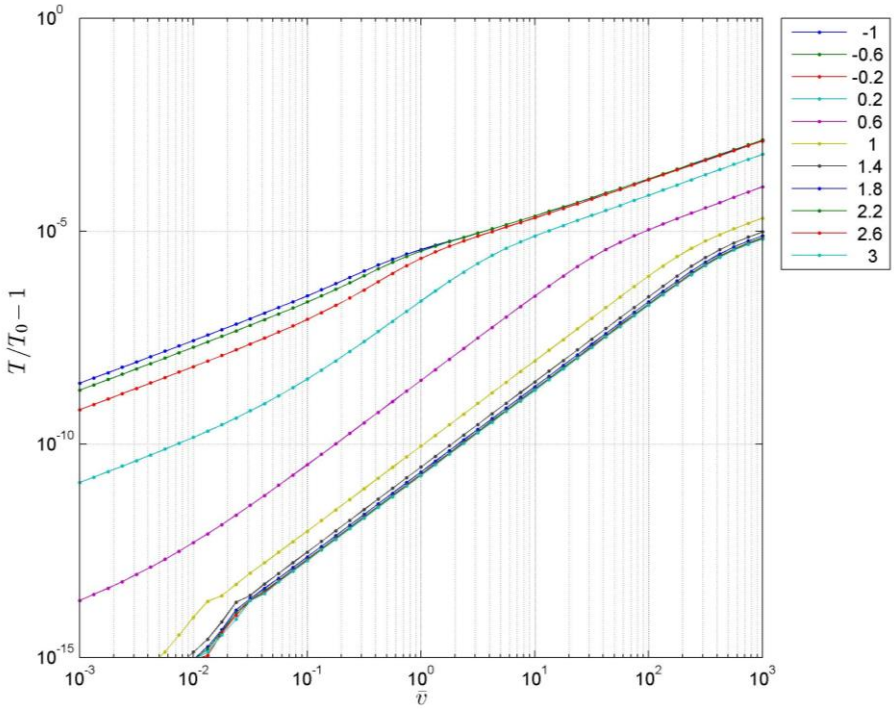

Fig. 5 Normalized shift of the temperature as a function of velocity for different Hurst exponents. Due to high normal force the elastomer is in full contact for low velocities. The slope is two. At higher velocities the contact becomes partial and the dependence is linear. This effect is occurs for lower Hurst exponents at lower velocities

3.2. Flash temperature

In each element, the energy dissipation leads to rise in temperature as stated above. For partial contact of the surfaces, the temperature will shift differently at contacting and non-contacting sites. Looking back at the motivation of this study we focus on the site of highest temperature. This temperature called flash temperature is the maximal temperature that we find over all sites. Certainly, it depends on the actual realization of the surface. Anyway, averaging over a large number of realizations (200 in our case) we find a rise of up to 5% of the temperature at a Hurst exponent of $H = 0.7$ as shown in Fig. 6.

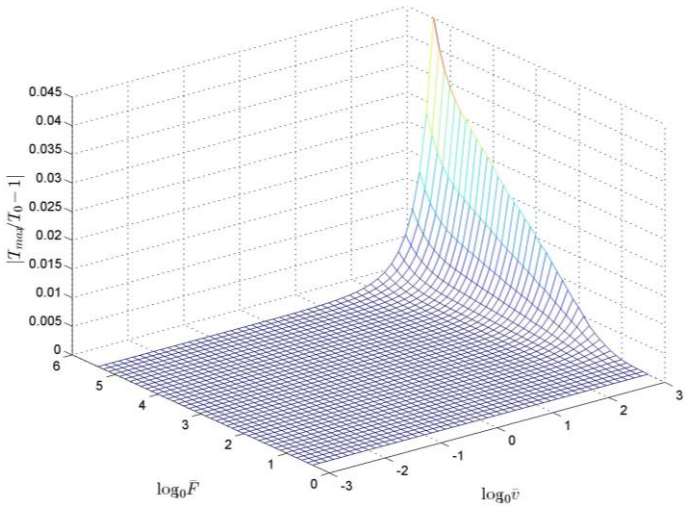

Fig. 6 Normalized shift of the flash temperature as a function of normalized velocity $\bar{v}$ and normalized normal force $\bar{F}$ at $H = 0.7$. For small velocities and forces the flash temperature shift is small but is enhanced for higher values of these quantities

As can be seen above the temperature shift is proportional to the power generated in each element. Looking for its highest value one has to distinguish between contact and non-contact sites. In non-contact sites the power is proportional to the difference between the coordinates squared. Obviously, this difference is largest when the detachment of the elastomer chain just occurred. The behavior of the free elastomer surface is governed by parameter dt/τ. In contact sites, the picture is different. Here, the elastomer surface follows the rigid profile. Hence it maps the surface topology of the rough surface into the dynamic behavior of the elastomer.

From Fig. 7 we see different behavior of the flash temperature depending on the contact configuration. For high normal force (LHS) the contacts saturate, i.e. there is full contact. The flash temperature shift increases with the normal load linearly. For lower loads, the relative contact number depends on the Hurst exponent of the rigid surface. On the right hand side, the normal force is held constant. Here the number of contacts is constant for low velocities. For higher speeds, more contacts are broken. For the flash temperature this means that, after having a linear dependence on the velocity, it saturates further on beginning for rough surfaces with a low Hurst exponent.

We propose the following power law dependencies of the flash temperature shift and the relative contacts

$$\begin{aligned} \left| \frac{T_{max}}{T_0} - 1 \right| &\propto \bar{v}^{\gamma_T} \bar{F}^{\delta_T} \\ \frac{N_{cont}}{N} &\propto \bar{v}^{\gamma_N} \bar{F}^{\delta_N} \end{aligned} \tag{57}$$

with the empirical exponents

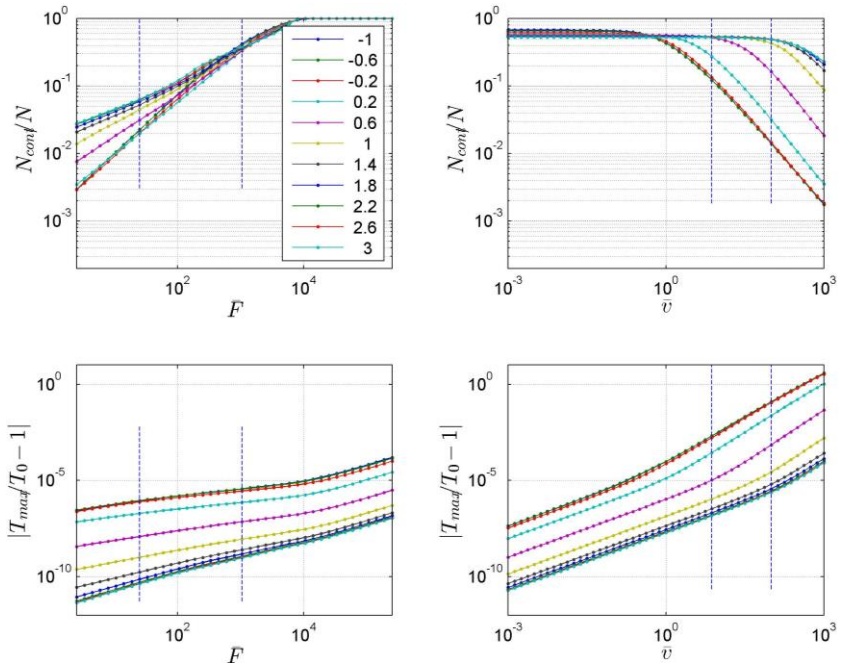

Fig. 7 Relative contacts (*Ncont* / *N*, upper row) and normalized shift of the flash temperature (lower row) as a function of normalized normal force $\bar{F}$ (left, velocity constant $\bar{v} = 0.1$) and normalized velocity $\bar{v}$ (right, normal force constant $\bar{F} = 0.5$) for different values of the Hurst exponent

$$\begin{aligned}
\gamma_T(H) &= \begin{cases} 1.6, & H \le 0 \\ 1.69 - 0.64H, & 0 \le H \le 1 \\ 1, & 1 \le H \le 3 \end{cases} \\
\delta_T(H) &= \begin{cases} 0.4, & H \le 0 \\ 0.32 + 0.26H, & 0 \le H \le 2 \\ 0.84, & 2 \le H \le 3 \end{cases} \\
\gamma_N(H) &= \begin{cases} -1, & H \le 0 \\ -0.87 + 0.84H, & 0 \le H \le 1 \\ 0, & 1 \le H \le 3 \end{cases} \\
\delta_N(H) &= \begin{cases} 0.8, & H \le 0 \\ 0.8 - 0.3H, & 0 \le H \le 1 \\ 0.5, & 1 \le H \le 3 \end{cases}
\end{aligned} \tag{58}$$

Fig. 8 shows the numerical fits of the slope, i.e. the exponents of the normalized normal force and velocity in the ranges as indicated in Fig.7.

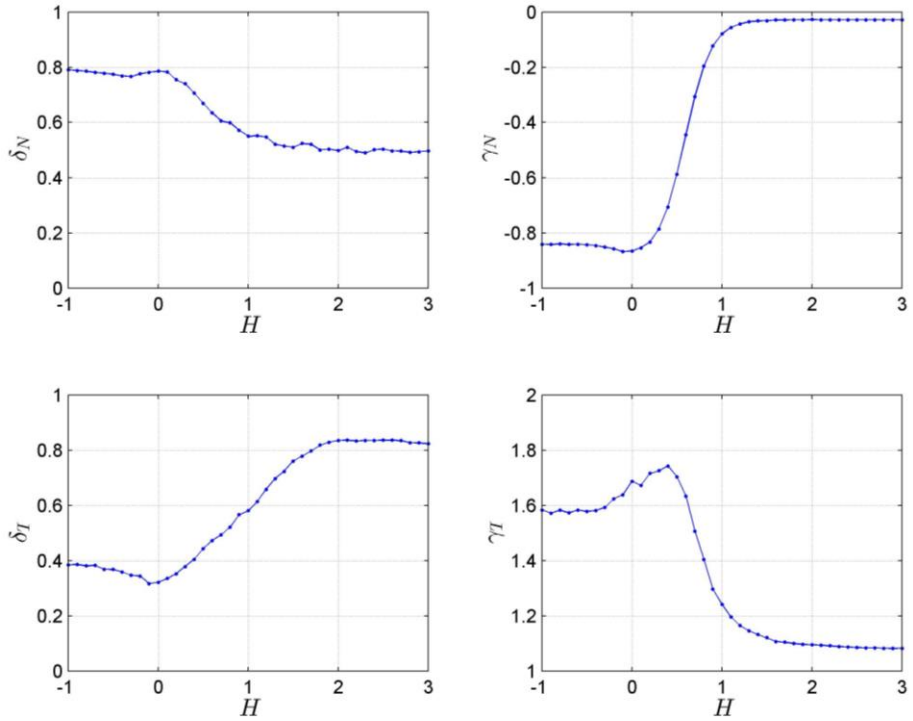

Fig. 8 Numerical fits of the exponents of normalized normal force (left, velocity constant) and normalized velocity (right, force constant) for relative contacts (upper row) and normalized shift of the flash temperature (lower row) in the power law Eq.(57) as a function of the Hurst exponent

The fit in the upper left corner resembles the result of Pohrt and Popov [23] for the purely elastic indentation. Furthermore, as already seen in Eq. (6), the most interesting range for the investigation of different Hurst exponents is [0,1]. For Hurst exponents up to 0, the flash temperature depends on the normal force with an exponent close to 0.4. In the intermediate range from 0 to 2, the exponent increases to 0.8. For constant forces (RHS), the flash temperature shift is depends on the velocity with an exponent of about 1.6 for low Hurst exponents. The exponent then decreases to values about 1 for Hurst exponents larger than 1.

4. Conclusions and Outlook

We have found in the framework of the MDR a strong implication that we can study the temperature dependence in the frictional contact of an elastomer with a rough surface in a simple Kelvin model. We have accomplished a shift in mean temperature as well in the flash temperature. The shift has been explored as a power law of the dimensionless normal force and velocity. The numerical fits of the exponents in the power laws have been carried out and the corresponding dependence on the Hurst exponent proposed. Further research can include more realistic elastomer models and lead to the temperature

dependence of the coefficient of friction itself. Furthermore a reduction of the parameter space by dimensionless quantities is appropriate.

Acknowledgements: *We are grateful to V. L. Popov and S. Kürschner for discussions. The author is financially supported by DFG project PO 810/12-2.*

REFERENCES

1. F. P. Bowden, D. Tabor, 1985, *The Friction and Lubrication of Solids*, Oxford University Press, p. 452.
2. J. A. Greenwood, D. Tabor, 1958, *The Friction of Hard Sliders on Lubricated Rubber: The Importance of Deformation Losses*, Proceedings of the Physical Society, 71, pp. 989-
3. K. A. Grosch, 1963, The Relation between the Friction and Visco-Elastic Properties of Rubber, Proceedings of the Royal Society, 274, pp. 21-39
4. M. Barquins, R. Courtel, 1975, *Rubber friction and the rheology of viscoelastic contact*, Wear, 32, pp. 133-150.
5. M. Klüppel, G. Heinrich, 2000, *Rubber Friction on Self-Affine Road Track*, Rubber Chemistry and Technology, 73, pp. 578-606.
6. B. N. J. Persson, 2001, *Theory of rubber friction and contact mechanics*, Journal of Chemical Physics, 115, pp. 3840-3861.
7. B. Lorenz, B. N. J. Persson, G. Fortunato, M. Giustiniano, F. Baldoni, 2013, *Rubber friction for tire tread compound on road surfaces, Journal of Physics: Condensed Matter*, 25, pp. 095007.
8. V. L. Popov, A. V. Dimaki, 2011, *Using Hierarchical Memory to Calculate Friction Force between Fractal Rough Solid Surface and Elastomer with Arbitrary Linear Rheological Properties*, Technical Physics Letters, 37, pp. 8-11.
9. A. Schallamach, 1952, *The Load Dependence of Rubber Friction*, Proceedings of the Physical Society. Section B, 65,pp. 657.
10. O. Ben-David, J. Fineberg, 2011, *Static Friction Coefficient Is Not a Material Constant*, Phys. Rev. Lett., 106, pp. 254301.
11. M. Otsuki, H. Matsukawa, 2013, *Systematic Breakdown of Amontons' Law of Friction for an Elastic Object Locally Obeying Amontons' Law*, Scientific Reports, 3, pp. 1586.
12. S. M. Rubinstein, G. Cohen, J. Fineberg, 2004, *Detachment fronts and the onset of dynamic friction*, Nature, 430, pp. 1005-1009.
13. O. Ben-David, G. Cohen, J. Fineberg, 2010, *The Dynamics of the Onset of Frictional Slip*, Science, 330, pp. 211-214.
14. D. S. Amundsen, J. Scheibert, K. Thögersen, J. Trömborg, A. Malthe-Sörenssen, 2012, *1D Model of Precursors to Frictional Stick-Slip Motion Allowing for Robust Comparison with Experiments*, Tribology Letters, 45, pp. 357-369.
15. M. Heß, 2011, *About Mapping of Some Three-dimensional Contact Problems to Systems with a Lower Spatial Dimensionality*, Cullier Verlag, Berlin.
16. M. Heß, 2012, *On the reduction method of dimensionality: The exact mapping of axisymmetric contact problems with and without adhesion*, Physical Mesomechanics, 15, pp. 264-269
17. R. Pohrt, V. L. Popov, A. E. Filippov, 2012, *Normal contact stiffness of elastic solids with fractal rough surfaces for one- and three-dimensional systems*, Phys. Rev. E, 86, pp. 026710.
18. V. L. Popov, M. Heß, 2015, *Method of Dimensionality Reduction in Contact and Friction*, Springer, Berlin Heidelberg.
19. Q. Li, M. Popov, A. Dimaki, A. E. Filippov, S. Kürschner, V. L. Popov, 2013, *Friction Between a Viscoelastic Body and a Rigid Surface with Random Self-Affine Roughness*, Phys. Rev. Lett., 111, pp. 034301.
20. A.V. Dimaki, V.L. Popov; 2014, *Coefficient of friction between a rigid conical indenter and a model elastomer: influence of local frictional heating*, Phys. Mech., 17 (5), p. 57-62.
21. V. L. Popov, 2010, *Contact mechanics and friction*, 1st ed., Springer, Berlin Heidelberg, 362 p.
22. I. A. Lyashenko, L. Pastewka, B. N. J. Persson, 2013, *Comment on "Friction Between a Viscoelastic Body and a Rigid Surface with Random Self-Affine Roughness"*, Phys. Rev. Lett., 111, 189401.
23. R. Pohrt, V.L. Popov, Valentin L., 2012, *Normal Contact Stiffness of Elastic Solids with Fractal Rough Surfaces*, Phys. Rev. Lett., 108, pp. 104301.